

Arrays of Ni/Co Nanoparticles within a Nanostructured Silicon Host

Klemens Rumpf, Petra Granitzer,* Roberto Gonzalez-Rodriguez, Jeffery Coffey, and Michael Reissner

Herein, nanostructured silicon is fabricated with two different embedded magnetic nanostructures (Ni/Co) to exploit the magnetic properties of both metals and discern the behavior of the exchange coupling between the two—especially with respect to their volume ratio. A variation of the size as well as the volume ratio of the two metals modifies the exchange coupling and thus the energy product. Two templates are utilized: one involves the use of porous silicon (PSi) and the other entails porous silicon nanotubes (SiNTs). In the case of PSi, the bimetallic structures (Ni/Co) are electrodeposited, whereas in the case of SiNTs, Co is chemically grown within the tubes followed by the deposition of Ni on the outside. The magnetic properties of the systems strongly depend on the geometry of the deposits, on the volume ratio of the two metals, as well as on the proximity of the deposits. If the distance is small enough magnetic exchange coupling is present. Due to their size and the coupling of the bimetallic structures, the switching behavior of the hysteresis can be varied. Ultimately, nanocomposites with an energy product as high as possible is achieved to give rise to applications as permanent nanomagnets.

within the porous structure, it is used as a sensor^[1] and furthermore acts as a template material for many kinds of materials such as polymers^[2] or metals.^[3] It is generally fabricated by etching (plus selected deposition steps) and thus involves relatively straightforward and low-cost processes. Template materials, such as porous alumina^[4] or porous silicon (PSi)^[5] which offers a 3D porous structure, are often used for electrodeposition of magnetic metals within the pores. The deposited nanostructures (particles, wires) have been investigated with respect to their magnetization reversal processes with the concomitant domain wall motion^[6] and the interactions among them.^[7] Transport phenomena like magnetoresistance in spin valves^[8] are also of great interest. Such nanocomposites offer specific magnetic properties depending on the size and the shape of the deposits as well as on the morphology of the

1. Introduction


Nanostructured silicon with its various morphologies is well known and used in many realms. By incorporating molecules

template used. In this study, two different kinds of magnetic metals are incorporated into the nanostructured silicon to exploit the specific properties of both and, under certain conditions, obtain the exchange coupling of bimetallic nanostructures. Exchange coupling between two different magnetic materials is often discussed for magnetic hard/soft materials.^[9] The usage of magnetic nanostructures composed of two different metals is of interest due to their tunable magnetic properties and their switching behavior. They are also investigated with respect to the fabrication of permanent nanomagnets. FePt and Fe₃O₄ nanoparticles have both been incorporated into binary assemblies where both the hard and the soft phases are controlled to ensure efficient exchange coupling.^[10] The best hard/soft geometries have been theoretically investigated with respect to achieving new permanent nanomagnet materials.^[11] To produce systems with broadly tunable magnetic properties, nanowires (such as segmented Co₅₄Ni₄₆/Co₈₅Ni₁₅) have been deposited, offering a specific magnetic switching behavior depending on the ratio of Co:Ni.^[12] In addition, hard/soft magnetic segmented nanowires consisting of Co/CoNi/Ni have been produced and investigated structurally and magnetically with the goal of controlling the movement of magnetic domain walls.^[13] While the fabrication of nanoscopic hard/soft magnetic structures is of intense interest, the processing requirements make it difficult to achieve the desired properties. The properties of the soft phase material are exploited to obtain an enhanced performance

Dr. K. Rumpf, Dr. P. Granitzer
Institute of Physics
University of Graz
Graz 8010, Austria
E-mail: petra.granitzer@uni-graz.at

Dr. R. Gonzalez-Rodriguez, Prof. J. Coffey
Department of Chemistry
Texas Christian University
Fort Worth, TX 76129, USA

Prof. M. Reissner
Institute of Solid State Physics
Vienna University of Technology
Vienna 1040, Austria

 The ORCID identification number(s) for the author(s) of this article can be found under <https://doi.org/10.1002/pssa.201901040>.

© 2020 The Authors. Published by WILEY-VCH Verlag GmbH & Co. KGaA, Weinheim. This is an open access article under the terms of the Creative Commons Attribution-NonCommercial-NoDerivs License, which permits use and distribution in any medium, provided the original work is properly cited, the use is non-commercial and no modifications or adaptations are made.

DOI: 10.1002/pssa.201901040

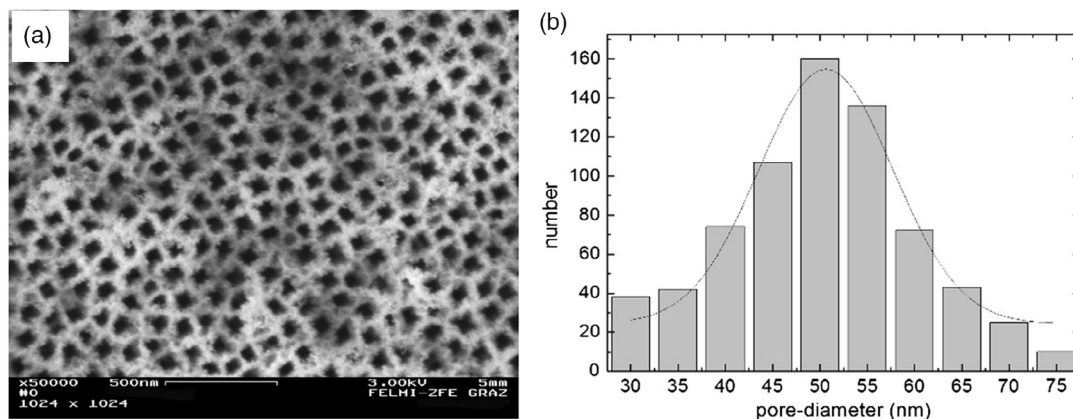


Figure 1. a) Top-view scanning electron micrograph showing a porous structure with an average pore diameter of 50 nm. b) Corresponding pore size distribution obtained from image processing.

compared with that of the bare hard magnetic material, which is generally the main component of the hard/soft magnetic nanostructure. The energy product of such structures is determined by the saturation magnetization of the soft phase and the coercivity of the hard phase.^[14] Due to their proximity, exchange coupling between these magnetic materials leads to an increase in the energy product. An increase in the coercivity can also be achieved by fabricating single-domain structures. It has been shown theoretically that the diameter of the soft phase structures should not exceed twice the domain wall thickness of the hard phase material.^[11] Furthermore, nanostructured systems consisting of layers of hard and soft magnetic thin films^[15] or core/shell particles with a hard magnetic core and soft magnetic shell^[16] are used to produce exchange coupled systems.

In this work, the fabrication of self-organized 3D arrays of magnetic nanostructures which are composed of two different metals (Ni and Co) is presented. The PSi and silicon nanotubes (SiNTs) act as the nonmagnetic matrix to achieve an arrangement of separated NiCo nanostructures. The goal is to utilize exchange coupling between these structures within individual pores/tubes by electrodeposition conditions and thus increase their energy product. In comparison with systems which consist of nanostructures of one metal, the energy product can be modified by adjusting the deposited amount of each of the two metals.

2. Experimental Section

2.1. PSi and SiNTs as Template Material

The PSi templates used in these experiments were produced by anodization of an n-type silicon wafer with 10 mΩ cm resistivity in a 10 wt% aqueous hydrofluoric acid solution. The applied current density was maintained constant at 100 mA cm⁻² during the etching process which resulted in a PSi morphology, offering average pore diameters of 50 nm and mean pore distances of 50 nm. The thickness of the porous layer depended on the etching time and resulted in a value of about 30 μm for these fabricated samples when an anodization time of 8 min was used. The pore-size distribution, gained from the image processing of top-view

scanning electron micrographs, showed a deviation of about 10% from the average pore diameter. Thus, the samples offered a mean porosity of 50%. **Figure 1a** shows a top-view scanning electron microscopy (SEM) image and in **Figure 1b**, the accompanying pore-size distribution is given. Further details on the fabrication procedure can be found in the study by Granitzer and Rumpf.^[17]

As an additional approach, SiNTs were used as a template material. The SiNTs were fabricated using a procedure reported previously by our research group.^[18] This process consisted of silicon deposition on a ZnO nanowire array used as a template, followed by removal of the ZnO core using an NH₃/HCl etch. **Figure 2** shows a transmission electron microscopy (TEM) image of such SiNTs.

In this work, magnetic nanostructures consisting of two different metals were deposited within nanostructured silicon to modify the magnetic switching behavior of the silicon/metal nanocomposite. The morphology (pore diameter of PSi, nanotube inner diameter) of the two systems, the PSi, and the SiNTs, was comparable. In the case of the PSi templates, a mesoporous morphology with a pore diameter in the range of 50 nm was used, and these pores were filled with two different

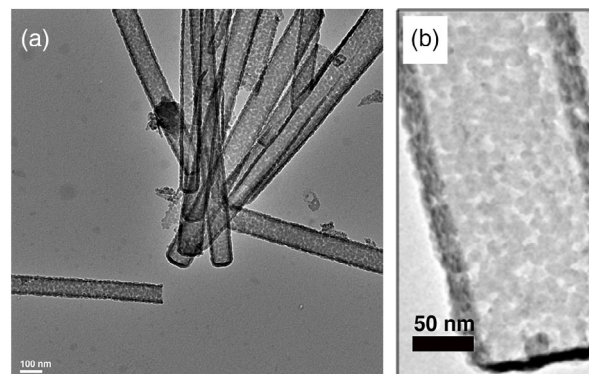


Figure 2. a) TEM image of SiNTs containing porous sidewalls ≈10 nm thick and an inner diameter ≈50 nm, fabricated by the sacrificial templating route described earlier. The scale bar shows 100 nm; b) a higher magnification image showing a porous structure (scale bar = 50 nm).

metals, namely Ni and Co. In the case of the SiNTs, the average inner diameter was 50 nm.

2.2. Ni/Co Deposition within Nanostructured Silicon

Metal deposition within the pores of PSi was performed by electrodeposition. In the case of depositing Ni and Co from separate electrolytes, aqueous NiSO₄ and CoSO₄ solutions were used. The composition of the Ni salt solution was 170 g L NiSO₄ and 40 g L H₃BO₃. For Co deposition, the electrolyte contained 120 g L CoSO₄ and 30 g L H₃BO₃. An applied current density of 15 mA cm⁻² and a frequency of 0.1 Hz were applied for 15 min. In the case of depositing Ni and Co from a single electrolyte, a solution in the ratio 1:1 of the Ni salt to Co salt was used. Ni was deposited by applying a potential of 1.1 V, and Co was deposited by changing to 1.8 V; the used deposition time of Co was three times longer than that for Ni (deposition time of Co: 15 min, deposition time of Ni: 5 min) to achieve a volume ratio Ni:Co = 1:7. A change of the deposition time to 5 min for Co and 5 min for Ni results in volume ratio of about Ni:Co = 1:3. The results were estimated from energy dispersive X-ray (EDX) investigations of the samples.

A complementary approach was the chemical growth of Co nanoparticles within porous SiNTs and the additional deposition of a Ni layer on the outer surface of the tubes. The inner diameter of the silicon tubes was around 50 nm, and the wall thickness was about 10 nm (Figure 2).

Cobalt nanoparticles (Co NPs) were formed in situ onto SiNTs. The initial step was the immersion of SiNTs in a solution containing 0.08 M of CoCl₂ · 6H₂O at room temperature; then 0.002 mol of NaBH₄ was added to the solution slowly with constant stirring. Finally, the Co NP-containing SiNTs were removed from the solution after 5 min, and the sample was washed several times with deionized (DI) water and ethanol. The additional Ni layer was deposited electrochemically using a Watts solution (45 g L NiCl₂, 300 g L NiSO₄, and 45 g L H₃BO₃) as electrolyte and applying a current density of 10 mA cm⁻² for 5 min.

As the wall of the silicon tubes offered a porous structure (Figure 2b), the Co particles, which were localized near the pore surface on the wall of a given nanotube, could touch the deposited Ni layer. An alternative structure involved the deposition of an

additional Si layer (after the growth of Co particles inside the tubes) as a spacer before Ni deposition to suppress the direct touching of Co particles and Ni layer. This additional Si layer of a few nanometers in thickness was produced by the same deposition process as the SiNTs itself (CVD with silane at 500 °C).

2.3. Magnetic and Structural Characterization

The magnetic characterization of the samples was conducted by a vibrating sample magnetometer (PPMS, Quantum Design). The measurements were carried out in dependence on the magnetic field between ±2 T.

The morphology of the deposited bimetal Ni/Co structures was analyzed by SEM and EDX. Figure 3a,b shows an SEM image and an EDX map of a cross section of a PSi sample filled with Ni and Co. The EDX map of Ni/Co deposits within PSi showed the distribution of Ni and Co; in this case (Figure 3b), the amount of Co dominates this image due to the longer deposition time (15 min deposition time of Co and 5 min deposition time of Ni, leading to a ratio Ni:Co 1:7).

In this way, the size and especially the volume ratio could be varied. For the aforementioned deposition times, the accompanying length of the Co component was ≈200 nm, and the Ni portion corresponded to a length of ≈30 nm. For all performed depositions, the concentrations of the Ni salt solution, the Co salt solution, and the Watts electrolyte were the same (as mentioned earlier). In addition, identical morphologies of PSi templates were used to minimize their structural and compositional effects on magnetic behavior. The deposition time was modified to change the size of the deposited nanostructures (e.g., a deposition of 5 min for Co and 5 min for Ni leads to a size of ≈100 nm for the Co component and ≈30 nm for the Ni component) as well as the volume ratio Ni:Co = 1:3 determined from EDX investigations.

3. Results and Discussion

Nanostructures which are composed of two different metals are fabricated by electrodeposition into a PSi framework using two distinct metal salt solutions or a single solution containing both

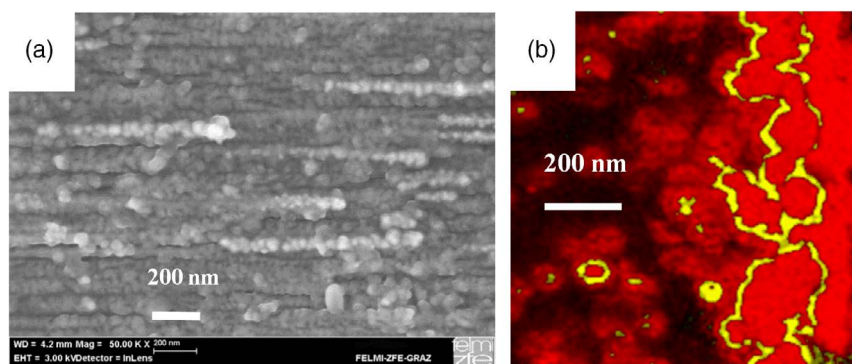


Figure 3. a) Cross-sectional SEM image of PSi filled with Ni/Co nanostructures. b) EDX map of a cross section of the same sample showing the Ni (yellow) and Co (red) distribution. The volume ratio between Co and Ni is about 1:7 = Ni:Co. Reproduced with permission.^[21] Copyright 2018, Electrochemical Society.

metal salts. These structures are used to vary the magnetic properties of the system, especially to enhance the energy product.

These two different deposition approaches have been used to fabricate such bimetal nanostructure arrays. In the first attempt where the two different ferromagnetic metals have been deposited alternatively from two metal salt solutions, one sees that the magnetic behavior is composed of two terms. The first term is mainly due to the one magnetic material, Ni, which exhibits a saturation magnetization of 0.6 T (bulk Ni). The second one is mainly due to the other magnetic material, Co, which exhibits a saturation magnetization of 1.7 T (bulk Co). Thus, the hysteresis curves of the investigated nanocomposite systems show two different slopes corresponding to the two different materials. First, up to a field of 500 Oe, the ferromagnetic behavior of Ni is dominant and above the saturation of the Ni structures; the behavior of the Co structures, which are saturated at higher fields, becomes more distinctive.

In the case of depositing both metals (Ni and Co) out of one electrolyte by changing the applied potential, a smooth hysteresis curve is observed. The coercivity increases to $H_C = 860$ Oe and the reduced remanence to $M_R/M_S = 0.64$ (Table 1), resulting in a higher energy product compared with single-metal deposition and to the deposition using two different metal salt solutions. This indicates that in the case of using a single-electrolyte bath exchange coupling between the two materials takes place because the structures of the two metals touch each other, whereas in the case of using two separate metal salt solutions, an oxide is presumably formed, thereby separating the two metals. The partial oxidation of the Ni/Co structures from two separate electrolytes is also shown by the shift of the coercivity after carrying out field-cooled magnetization measurements. Before the measurements, the sample is heated to 300 K and then cooled to 4 K. The resulting hysteresis of this measurement shows an asymmetric coercivity (of ≈ -500 Oe and $+200$ Oe), which is shown in Figure 4. In the case of Ni/Co deposition from a single electrolyte, this shift of the coercivity is not observed.

Figure 5 shows the field-dependent magnetization of Ni and Co deposited within PSi using a single-electrolyte solution and changing the applied potential from 1.1 to 1.8 V. This is compared with the sample produced from two separate electrolytes. The dotted line represents the deposition of the Ni/Co structures from two metal salt solutions. The full line corresponds to the deposition from a single-electrolytic bath. The hysteresis curves of the Ni/Co composite systems are measured at room temperature.

Figure 6 shows for comparison a hysteresis curve of Ni filled within PSi (a) and Co deposited within PSi (b). The slopes of the two curves correspond to the sample in Figure 5 containing Ni as well as Co deposited from two separate electrolytes (dotted line),

Table 1. Coercivity and squareness (magnetic remanence M_R /saturation magnetization M_S) of different metal depositions into PSi.

Metal	Coercivity [Oe]	Squareness [M_R/M_S]
Ni	300 ^[22]	0.28
Co	450 ^[23]	0.13
Ni/Co (2 electrolytes)	520	–
Ni/Co (1 electrolyte)	860	0.64

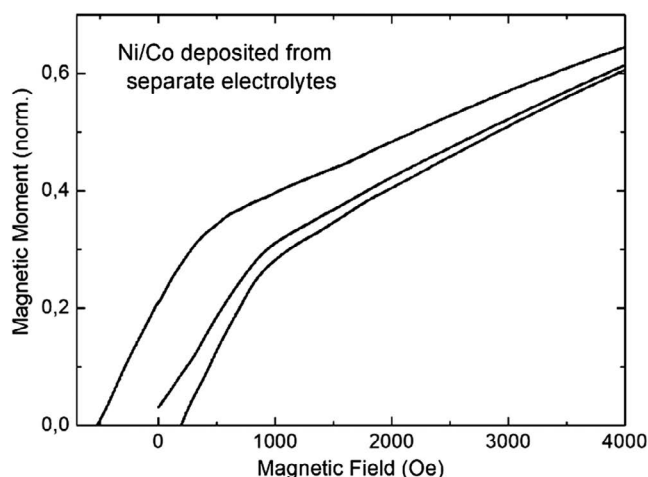


Figure 4. Field-cooled magnetization measurement (sample heated to 300 K and then cooled to 4 K prior to the measurement) showing an asymmetric hysteresis curve (positive part) with the initial magnetization curve starting close to 0 (middle), the downward curve after saturation (left), and the upward curve back to saturation (right). This asymmetric behavior is attributed to metal oxide formation during the deposition process. Metal deposition is performed from two separate electrolytes.

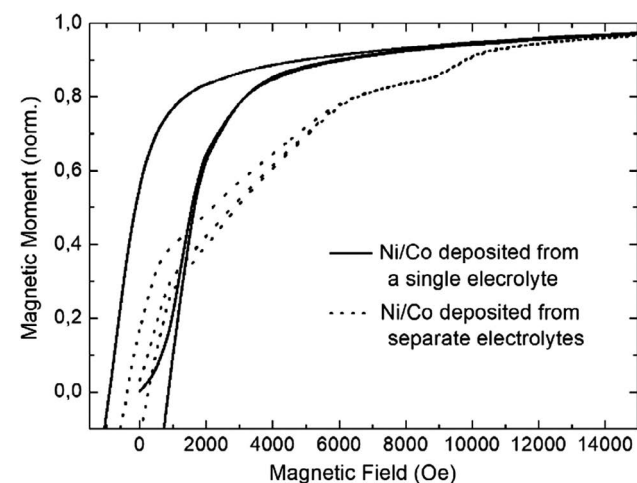


Figure 5. A comparison of field-dependent magnetization measurements of Ni/Co nanostructures deposited within PSi from two metal salt solutions (dotted line) and from a single electrolyte (full line). The sample produced from a single electrolyte offers higher coercivity due to the higher proximity of the Ni and Co nanostructures, leading to exchange coupling between them. The measurements have been carried out at 300 K.

offering two slopes of each component. This comparison shows that in the case of using two electrolytes for bimetal deposition there is no exchange coupling between the deposits and therefore the magnetic response of the two metals can be recognized.

For the magnetization measurements of the PSi containing nanostructures of only one metal (Ni or Co), the coercivity and the remanence are determined by the shape and the size of the metal deposits (obtained by back-scattered electron micrographs), and they are lower compared with samples containing

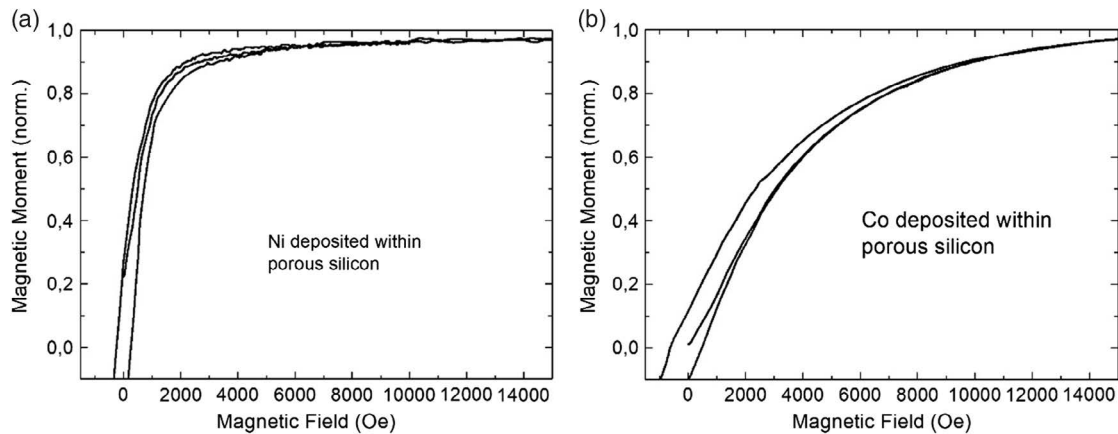


Figure 6. Field-dependent magnetization curves of a) Ni-filled PSi and b) Co-filled PSi. The measurements have been carried out at 300 K.

nanostructures composed of two metals. The deposition times in both cases are the same (single-electrolyte and two-electrolyte deposition) for Ni and Co, and also from observed EDX spectra (not shown here), similar length can be assumed, whereas the diameter of the structures is concomitant to the pore diameter. In Table 1, the coercivities (H_C) and the reduced remanence (M_R/M_S) of Ni-, Co-, and NiCo-filled PSi are listed.

The measurements have been carried out at $T = 300$ K. For the sample prepared from two separate electrolytes, the squareness cannot be provided as the magnetization curve yields two different slopes. The combination of both metals leads to an enhancement of these magnetic properties due to exchange coupling between the two different metal structures.

Considering the coercivity of the PSi/NiCo nanocomposites, one sees that H_C increases with increasing Co deposition time, maintaining the deposition time of Ni constant at 5 min (Table 2).

The bimetal structures lead to an enhanced coercivity and remanence compared with the single-metal nanostructures. The sizes of the Co and the Ni structures are crucial with respect to the resultant magnetic properties. Preferable are nanostructures as small as possible but big enough that the thermal energy does not predominate and overwhelm the magnetic ordering of the material. In this work, the size of the Co component of the deposited bimetal nanostructures is ≈ 200 nm, and the size of the Ni component is around 30 nm. The diameter of the deposited metal structures generally corresponds to the pore diameter (≈ 50 nm) of the used matrix. The elongation depends on the electrochemical deposition parameters.^[19]

By varying the amount of Ni and Co, respectively, in changing the deposition time, the coercivity and the remanence can be

Table 2. Coercivity of PSi/NiCo nanocomposites versus the deposition time of Co.

Coercivity [Oe]	Deposition time of Co [min]
580	5
710	10
860	15

adjusted, and thus the energy product of the system. For a sample with Ni and Co deposited from one electrolyte (Ni 5 min, Co 15 min; volume ratio Ni:Co = 1:7), an energy product $(BH)_{\max}$ of ≈ 26 MGOe has been estimated^[16] using $(2\pi M_S)^2$. It is about 44% and 24% higher than using bare Ni or bare Co which offers a $(BH)_{\max}$ of 18 and 21 MGOe, respectively. Changing the volume ratio of the involved metals to Ni:Co = 1:3, an energy product of about 19 MGOe is achieved which is close to the gained $(BH)_{\max}$ of Ni. In addition to magnetostatic interactions taking place between neighboring bimetal nanostructures, exchange coupling between the Ni and Co parts is essential for varying the magnetic properties of the nanocomposite. In a previous work,^[20] it has been shown that PSi filled with Ni nanostructures offers magnetostatic interactions dependent on the PSi morphology, especially the thickness of the remaining silicon skeleton between the pores. Thus magnetostatic interactions also occur in the investigated samples. Generally dipolar coupling between adjacent nanostructures leads to a decrease in the coercivity.

In the case of SiNTs infiltrated with metal nanoparticles such as Co, TEM confirms the presence of Co nanoparticles and their location within the outer layer of the nanotube (Figure 7), in this case synthesized within the sidewall nanopores by chemical reduction of a metal salt.

Figure 8 shows SEM images of Co-filled SiNTs with the according Co particle size distribution. Synthetically, the Ni can be formed directly on top of the Co layer, or alternatively as pointed out earlier, a Si buffer layer can be grown over the Co NPs prior to Ni formation.

Figure 9 shows an SEM image of SiNTs with synthesized Co particles and an additional Ni layer outside covering the tubes.

Figure 10 shows a comparison of the field-dependent magnetic moments for different SiNT configurations with Co and Ni, namely SiNTs with incorporated Co particles and an additional Ni layer covering the tubes outside with or without a Si spacer layer and SiNTs only with Ni layer.

A comparison of the magnetic response of these three types of samples makes apparent the differences of their magnetic characteristics. An accurate analysis gives a coercivity (H_C) of about 150 Oe for SiNTs with only Ni deposited on the outer walls.

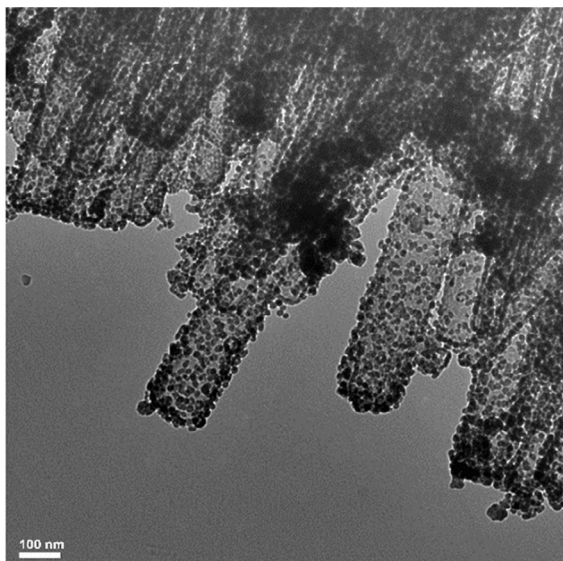


Figure 7. TEM image of porous SiNTs possessing embedded Co nanoparticles along the side walls of the nanotubes. The average tube walls are 10–20 nm, the average inner diameter is in the range of 50–60 nm. The scale bar shows 100 nm.

SiNTs with both, Co particles grown inside the walls and Ni deposited on the outer walls, offer a coercivity of about 290 Oe. An H_C of about 220 Oe is measured for SiNTs with Co particles grown inside, an additional Si spacer deposited

on the outer walls, and finally Ni deposited on the silicon spacer. Therefore the distance between the Co particles inside the tubes and the Ni layer on the outside varies depending on whether a silicon spacer is given or not. The results show that the variation of the proximity of the Co NPs and Ni layer modifies the coercivity of the systems. In the case of a no silicon spacer, an increase in the energy product can be reached, by choosing two kinds of metals (hard/soft magnetic materials), which is a hint that the already weak exchange coupling between the two different metals is present. Considering the samples containing an additional silicon spacer between Ni and Co, a two-slope behavior could not be observed, which is due to the dominance of one metal, namely Ni, which is electrodeposited on the outer tube walls.

4. Conclusions

In this work, the dependence of the magnetic properties of a nanostructured silicon/bimetal nanocomposite on the volume ratio of the metals, the proximity of the incorporated nanostructures (with and without an oxide layer), and also the size of the metal deposits have been determined. Furthermore, the presence of exchange coupling between the two different metal (Ni, Co) nanostructures could be observed for both template strategies. By varying bimetal deposition an energy product higher than for either of the single metals can be achieved.

Metal nanostructures consisting of Ni and Co have been electrochemically deposited within P*Si*. The deposition has been conducted by two routes, first, the deposition from two metal salt

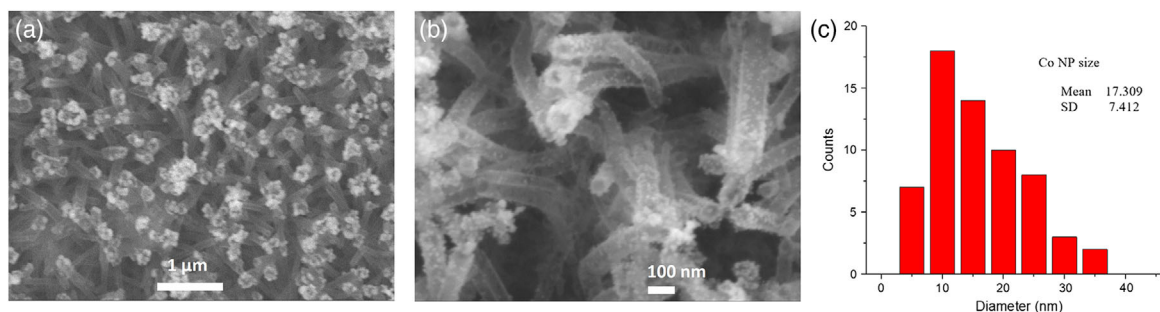


Figure 8. a,b) SEM images of Co nanoparticle-modified SiNTs. c) The corresponding Co nanoparticle size distribution.

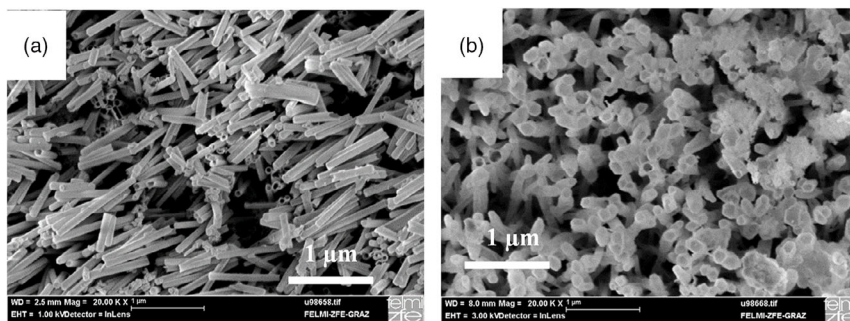


Figure 9. a) Bare SiNTs; b) SiNTs with Co nanoparticles grown inside, and an additional Ni layer on the outer tube walls (Co inside the tubes cannot be seen here). (Remark: Only Ni deposited on the SiNTs looks the same as the Ni covers the tube outside).

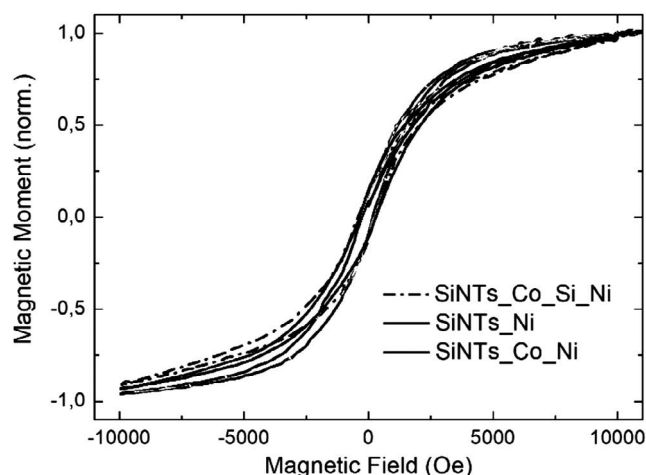


Figure 10. A comparison of magnetization curves of SiNTs with a Ni layer covering the outer tube wall (full line), incorporated Co particles and an additional Ni layer (dotted line), and incorporated Co particles with a Si spacer between the additional Ni layer (dashed line). The measurements have been carried out at 300 K.

solutions and second, the deposition from a single electrolyte consisting of both metal salts. In using two distinct electrolytes for the deposition of the two metals, the hysteresis curve shows a clear kink due to the different switching behaviors of Ni and Co. In using a single-electrolyte solution, the gained magnetization curve is smooth, and the coercivity and the remanence are enhanced compared with the single deposition of either Ni or Co. This result shows exchange coupling between the two metals. Furthermore, the deposition time of the two metals has been varied. By choosing deposition times of 15 min for Co and 5 min for Ni, the best results have been obtained, offering a coercivity of about 860 Oe and a reduced remanence of about 0.64. The size of the metal structures as well as their volume ratio plays a crucial role in maximizing the energy product and thus has to be modified accurately. Furthermore, the morphology of the porous silicon plays an important role as it affects dipolar coupling between metal structures in adjacent pores. If effectual dipolar coupling is present, the coercivity is reduced as it also affects the energy product. Due to the dendritic pore growth in a 3D array, dipolar coupling cannot be neglected which decreases the $(BH)_{\max}$ of the samples due to a reduction of the mean distance between the pores and appearing stray fields.

When using SiNTs as a template material, exchange coupling of incorporated Co particles with an outer Ni layer can be achieved. Furthermore, the magnetic properties can be modified by depositing a spacer Si layer in between the Co structures and Ni. So far, the Ni layer offers a thickness which leads to a dominance of Ni in the magnetic response but it could be shown that a variation of the proximity of the involved metals, Ni and Co, leads to significant differences in the hysteresis of the sample and an increase in the energy product.

The control of the size and volume ratio of hard/soft magnetic metal structures within nanostructured silicon could be shown to be a precondition to fabricate the 3D arrays of permanent nanomagnets within such templates.

Acknowledgements

The authors thank the Institute for Electron Microscopy at the University of Technology Graz for selected SEM measurements and the Institute of Solid State Physics at the Vienna University of Technology for the possibility to carry out magnetization measurements. Financial support by the Robert A. Welch Foundation (grant P-1212 to JLC) is also gratefully acknowledged.

Conflict of Interest

The authors declare no conflict of interest.

Keywords

magnetic nanoparticles, metal deposition, porous silicon, silicon nanotubes

Received: December 18, 2019

Revised: January 30, 2020

Published online: February 23, 2020

- [1] G. A. Rodriguez, J. D. Ryckman, S. M. Weiss, *Biosens. Bioelectron.* **2014**, *15*, 486.
- [2] K. Fukami, T. Sakka, Y. H. Ogata, T. Yamauchi, N. Tsubokawa, *Phys. Status Solidi A* **2009**, *206*, 1259.
- [3] Y. H. Ogata, K. Kobayashi, M. Motoyama, *Curr. Opin. Solid State Mater. Sci.* **2006**, *10*, 163.
- [4] M. Susano, M. P. Proenca, S. Moraes, C. T. Sousa, A. P. Araujo, *Nanotechnology* **2016**, *27*, 335301.
- [5] P. Granitzer, K. Rumpf, *Semicond. Sci. Technol.* **2016**, *31*, 014004.
- [6] J. Grollier, A. Chanthbouala, R. Matsumoto, A. Anane, V. Cros, F. Nguyen van Dam, A. Fert, *C. R. Phys.* **2011**, *12*, 309.
- [7] M. Pardavi-Horvath, *Phys. Status Solidi A* **2014**, *211*, 1030.
- [8] I. Ennen, D. Kappe, T. Rempel, C. Glenske, A. Hütten, *Sensors* **2016**, *16*, 904.
- [9] A. Lopez-Ortega, M. Estrader, G. Salazar-Alvarez, A. G. Roca, J. Nogues, *Phys. Rep.* **2015**, *553*, 1.
- [10] H. Zeng, J. Li, J. P. Liu, Z. L. Wang, S. Sun, *Nature* **2002**, *420*, 395.
- [11] R. Skomski, P. Manchanda, P. Kumar, B. Balamurugan, A. Kashyap, D. J. Sellmyer, *IEEE Trans. Mag.* **2013**, *49*, 3215.
- [12] V. M. Prida, J. Garcia, L. Inglesias, V. Vega, D. Görlitz, K. Nielsch, E. D. Barriga-Castro, R. Mendoza-Resendez, A. Ponce, C. Luna, *Nanoscale Res. Lett.* **2013**, *8*, 263.
- [13] A. Pereira, J. L. Palma, M. Vazquez, J. C. Denardin, J. Escrig, *Phys. Chem. Chem. Phys.* **2015**, *17*, 5033.
- [14] R. Skomski, J. M. D. Coey, *Permanent Magnetism*, Institute of Physics Publishing, Bristol, Philadelphia **1999**.
- [15] F. Liu, Y. Hou, S. Gao, *Chem. Soc. Rev.* **2014**, *43*, 8098.
- [16] Y. Liu, D. J. Sellmyer, *AIP Adv.* **2016**, *6*, 056010.
- [17] P. Granitzer, K. Rumpf, *Materials* **2010**, *3*, 943.
- [18] X. Huang, R. Gonzalez-Rodriguez, R. Rich, Z. Gryczynski, J. L. Coffey, *Chem. Commun.* **2013**, *49*, 5760.
- [19] K. Rumpf, P. Granitzer, P. Pölt, H. Krenn, *ECS Trans.* **2009**, *16*, 83.
- [20] P. Granitzer, K. Rumpf, T. Ohta, N. Koshida, M. Reissner, P. Poelt, *Appl. Phys. Lett.* **2012**, *101*, 33110.
- [21] K. Rumpf, P. Granitzer, H. Michor, P. Poelt, *ECS Trans.* **2018**, *85*, 1349.
- [22] K. Rumpf, P. Granitzer, N. Koshida, P. Pölt, M. Reissner, *Nanoscale Res. Lett.* **2014**, *9*, 412.
- [23] K. Rumpf, P. Granitzer, M. Reissner, P. Poelt, *ECS Trans.* **2012**, *41*, 59.